Comparative study of the electronic structure of two laser crystals: $BeAl_2O_4$ and $LiYF_4$

W. Y. Ching* and Yong-Nian Xu
Department of Physics, University of Missouri-Kansas City, Kansas City, Missouri 64110

B. K. Brickeen
Honeywell FM & T, Kansas City, Missouri 64141

(Received 29 September 2000; published 20 February 2001)

The ground-state electronic structure and bonding of two important laser crystals, $BeAl_2O_4$ and $LiYF_4$, were calculated using a first-principles method based the local approximation of the density-functional theory. The results were compared with similar calculations on several other laser crystals including yttrium aluminum garnet ($Y_3Al_5O_{12}$). The geometry of each crystal was optimized first with all internal parameters relaxed. The bulk moduli B were obtained by fitting the calculated total energies at different volumes to the Murnaghan equation of state. It was found that $LiYF_4$ ($B=90.0$ GPa) is much softer than $BeAl_2O_4$ ($B=217.3$ GPa). In $BeAl_2O_4$, Be and Al atoms have very similar local electronic structure and the crystal resembles that of α-Al_2O_3 (sapphire). $LiYF_4$ is a highly ionic crystal while $BeAl_2O_4$ has a significant amount of covalent mixing. The density of states, their atomic and orbital decompositions, the effective charges, the bond order, and the charge distributions in these two crystals are presented and contrasted.

DOI: 10.1103/PhysRevB.63.115101 PACS number(s): 71.20.Ps

I. INTRODUCTION

The development of solid-state laser technology depends on two critical ingredients: a robust crystalline or glassy medium and a suitable doping element. The doping ion is usually a rare-earth element or a transition-metal ion that can produce desired localized levels in the gap of the host crystal for emission and absorption at specific frequency ranges. Among a variety of laser crystals, oxides with a garnet structure such as yttrium aluminum garnet ($Y_3Al_5O_{12}$), or YAG, occupy the most prominent position because of their superior physical properties such as hardness, low index of refraction, resistance to optical damage, and chemical inertness. The Nd:YAG laser is therefore unquestionably the most well-known laser in commercial market. Other laser host crystals include sapphire (α-Al_2O_3), magnesia (MgO), spinel ($MgAl_2O_4$), forsterite ($MgSi_2O_4$), and several fluorides.[1,2] Most theoretical studies on laser crystals concentrated primarily on the spectroscopy of the energy levels of the doping element in the local environment of a given host material, developed in the framework of the ligand field theory.[3–5] The atomic multiplet levels were typically calculated with crystal-field parameters fixed by experimental data, while the physical properties of the host itself were frequently ignored. In particular, the electronic structure and bonding in many laser crystals have not been extensively studied, while such investigations can contribute to the understanding of many salient features of laser operation and may even aid to the discovery of new laser host materials.

Recently, we have studied the electronic structure and bonding of several laser crystals with a garnet structure: GSGG ($Gd_3Sc_2Ga_3O_{12}$), GSAG ($Gd_3Sc_2Al_3O_{12}$), and GGG ($Gd_3Ga_5O_{12}$),[6] in addition to the earlier study on YAG.[7] The difference in chemical bonding of cations of various sizes at the tetrahedral and the octahedral sites in the garnet structure was emphasized. Over the years, our group had studied the electronic structure and optical properties of many ceramic crystals, which are also laser-host materials, such as α-Al_2O_3,[8,9] $MgAl_2O_4$,[9] MgO,[9] $YAlO_3$,[10] and CaF_2.[11] Several other groups have also studied many laser crystals using different methods.[12–16] In this paper, we extend our study to two important laser crystals, $BeAl_2O_4$ and $LiYF_4$ (YLF). To our knowledge, the electronic structure and boding of these two crystals have never been reported. $BeAl_2O_4$ is a beautiful gemstone. When doped with Cr^{3+}, it is an effective laser material called alexandrite, whose discovery in the 1970s spurred a flurry of activities in the laser community[17] and had led to the further development of tunable vibronic lasers. YLF is the paradigm of the fluoride-based laser materials with Nd:$LiYF_4$ the most successful fluoride-based laser. Other fluoride-based laser crystals include CaF_2, LiCaF, $LiCaAlF_6$, and fluoral apatite [$Ca_5(PO_4)_3F$].[1] Generally speaking, oxide laser crystals have better thermomechanical properties while fluoride laser crystals have lower thermal lensing distortion. A comparative study of the electronic structure of these two crystals is particularly interesting because it contrasts an oxide with a fluoride. Furthermore, the four cations and the two anions in these two crystals are distinctively different, and so are their crystal structures. By comparing the electronic structure results of these two crystals in conjunction with others already studied, a consistent overall picture on the electronic properties of laser crystals in general can be obtained.

In the following section, Sec. II, we describe the crystal structure of $BeAl_2O_4$ and $LiYF_4$. We briefly outline the method of calculation in Sec. III. The main results on the ground-state properties, the electronic structure, and bonding are presented and discussed in Sec. IV. In the last section, Sec. IV, we make some concluding remarks and comment on the direction of future investigations.

II. CRYSTAL STRUCTURE

The crystal structure of $BeAl_2O_4$ and $LiYF_4$ are sketched in Fig. 1. The lattice constants and the interatomic distances

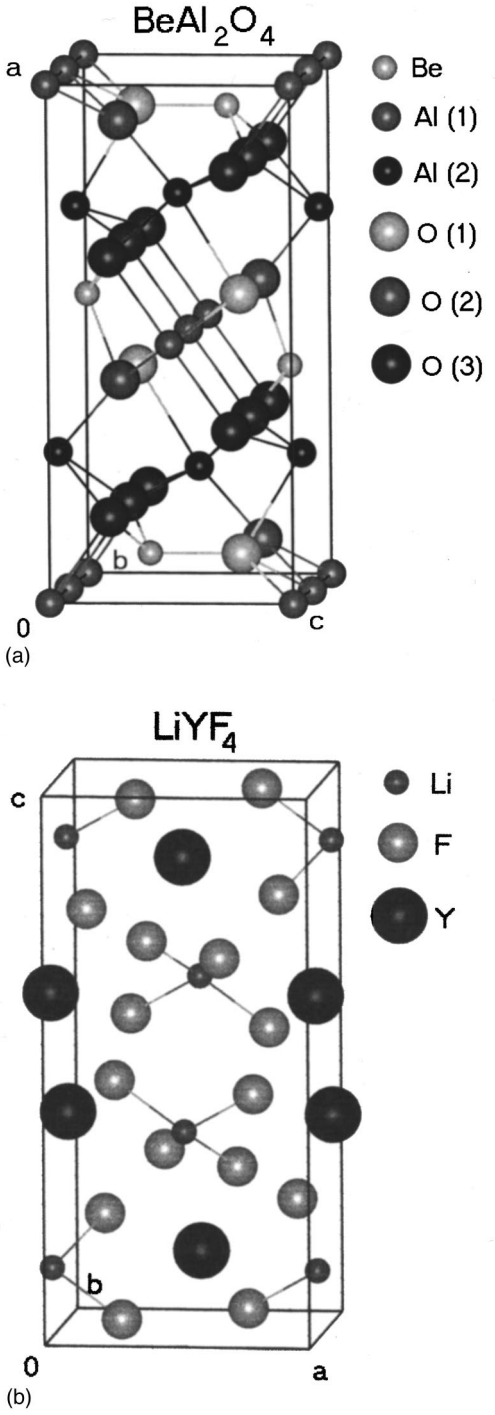

FIG. 1. Crystal structure of $BeAl_2O_4$ and $LiYF_4$.

are listed in Table I. The perfect crystal $BeAl_2O_4$ is the mineral chrysoberyl. Chrysoberyl can be regarded as a close-packed analog to the spinel structure and is isomorphic with olivine. The gemstone alexandrite is a Cr-doped variation of chrysoberyl. It has an orthorhombic cell with a space group of *Pnma*. The crystal structure was refined by Farrel, Fang, and Newnham,[18] based on the earlier measurement of Bragg and Brown.[19] There are two nonequivalent Al sites (denoted by Al1 and Al2) and three O sites (denoted as O1, O2, and O3). Both Al ions are octahedrally coordinated with Al-O bond lengths (BL) ranging from 1.861 to 2.017 Å (see Table I). This is to be compared with the Al-O BL of 1.857 and 1.967 Å in α-Al_2O_3, and the Al-O BL of 1.761 Å (tetrahedral site) and 1.937 Å (octahedral site) in YAG. The Be atom is tetrahedrally coordinated with relatively short Be-O BL's of 1.579, 1.631, and 1.687 Å. Al1 and Al2 have local point group symmetry of *Cs* and *Ci*, respectively, commonly referred to as the mirror site and the inversion site. The substitution of Cr^{3+} in alexandrite is predominately at the mirror site Al1.[20]

The $LiYF_4$ crystal is obtained from equimolar mixing of LiF and YF_3. The tetragonal cell belongs to the space group $I4_1/a$ with four formula units per cell.[21,22] The crystal is birefringent since it has a scheelite structure. The as-grown crystal contains a significant amount of rare-earth impurities so the structure for a pure $LiYF_4$ may be slightly different. The Li ion has four and the Y ion has eight nearest-neighbor (NN) F ions. The two Y-F NN distances of 2.244 and 2.297 Å are much larger than the single Li-F NN distance of 1.897 Å. On the other hand, Y in YAG is also dodecahedrally coordinated but the Y-O distances of 2.303 and 2.432 Å are considerably larger than the Y-F distances in YLF.

III. METHOD OF CALCULATION

As with other previous studies on laser crystals and inorganic optical materials, we used the *ab initio* orthogonalized linear combination of atomic orbitals (OLCAO) method[23] for the electronic structure calculation. Here, we only outline the details that are pertinent to the present calculation. In the OLCAO method, the basis expansion consists of atomic orbitals, which are expressed in terms of Gaussian types of orbitals.[23] For $BeAl_2O_4$, the basis set consists of Be $\underline{1s}$,$2s$,$3s$,$\underline{2p}$,$3p$, Al $\underline{1s}$,$2s$,$3s$,$4s$,$\underline{2p}$,$3p$,$4p$,$3d$, and O $\underline{1s}$,$2s$,$3s$,$\underline{2p}$,$3p$ atomic orbitals. For $LiYF_4$, it consists of Li $\underline{1s}$,$2s$,$3s$,$2p$,$3p$; Y $\underline{1s}$,$\underline{2s}$,$\underline{3s}$,$\underline{4s}$,$5s$,$6s$,$\underline{2p}$,$\underline{3p}$,$4p$,$5p$, $\underline{3d}$,$4d$,$\underline{5d}$ atomic orbitals. These basis sets are generally referred to as full basis sets. A minimal basis set in $BeAl_2O_4$ will have Be $3s$,$3p$, Al $4s$,$4p$, and O $3s$,$3p$ removed from the full basis set. Similarly, a minimal basis set in $LiYF_4$ will have Li $3s$,$3p$, Y $6s$,$5d$, and F $3s$,$3p$ removed from the full basis set. The core orbitals (those underlined) were orthogonalized to the ''noncore'' orbitals and later eliminated from the secular equation. The semicore Y $4p$ orbital in $LiYF_4$ was treated as a noncore orbital. The crystal potentials were constructed according to the density-functional theory with the local density approximation (DFT-LDA).[24] The Wigner-interpolation formula was employed to account for additional correlation effect in the LDA potential. The crystal potentials were written as a superposition of atom-centered functions each consisting of a combinations of *s*-type Gaussians. Full lattice convergence was obtained and no restrictions were imposed on how far the interactions of distant atoms should be included. Experimental lattice constants were used for the electronic structure calculation, although the geometry of the crystal structures was separately optimized by minimization of the LDA total energy. Geometry optimization is necessary in order to obtain the accurate bulk modulus using total energy values obtained from the OLCAO-LDA calculation.

TABLE I. Crystal parameters and interatomic distances in $BeAl_2O_4$ and $LiYF_4$. The number in the parentheses indicates the number of bonds.

Crystals	$BeAl_2O_4$	$LiYF_4$
Space group	*Pnma*	$I4_1/a$
Lattice constants		
a (Å)	9.404	5.164
b (Å)	5.476	
c (Å)	4.424	10.741
Cation coordination	4 (Be), 6 (Al)	4 (Li), 8 (Y)
Cation-anion distance	Be-O: 1.579, 1.687, 1.631 (2)	Y-F: 2.244 (4), 2.297 (4)
	Al1-O: 1.861 (2), 1.892 (2), 1.917 (2)	Li-F: 1.897 (8)
	Al2-O: 1.941 (2), 1.862(2), 1.893, 2.017	

The computational scheme for geometry optimization has been well described in recent publications.[25,26] For effective charge and bond order calculations, separate minimal-basis-set calculations consisting of only the valence-shell orbitals (including the Al $3d$ in $BeAl_2O_4$) were carried out. A sufficiently large number of k points was used both in the self-consistent iterations of the crystal potential and in the final analysis of the density of states (DOS).

IV. RESULTS

A. Bulk properties

The crystal structures of $BeAl_2O_4$ and $LiYF_4$ were optimized by the energy minimization scheme described before.[25,26] Both the lattice constants and the internal parameters were varied as the total energy converged to a minimum. The resulting equilibrium lattice constants and volumes are listed in Table II. The theoretical values are within 0.6% to 0.8% of the measured values listed in Table I. This is well within the accuracy of calculations based on density-functional theory. No attempts were made to improve the agreement by using other forms of the extension to the LDA theory, such as the popular generalized gradient approximation (GGA).[27] For ionic crystals, there is no convincing evidence that GGA can actually improve the agreement in the equilibrium lattice structure. Part of the disagreement in the lattice constants for YLF can be attributed to the doped nature of the crystal while the calculation is for a perfect dopant-free crystal. The same minimization scheme applied to the three known crystalline phases of Si_3N_4 (Ref. 25) and several complex oxides (Ref. 26) such as YAG, Al_2O_3, $MgAl_2O_4$, MgO, Y_2O_3, and $YAlO_3$ yielded considerably better agreement in the equilibrium geometry.

The total energies E of $BeAl_2O_4$ and YLF at different and fixed volumes V were calculated with all internal parameters relaxed. Eight E vs V data points in the range of lattice expansion up to 1.5% and contraction down to -2.0% were obtained and fitted to the Murnaghan equation of state (EOS).[28] Figure 2 shows the calculated data points and the fitted EOS for the two crystals. The bulk moduli B and the pressure coefficients B' for the two crystals are listed in Table II. For $BeAl_2O_4$, the calculated B of 217.2 GPa is comparable to that of α-Al_2O_3 (248 GPa) and YAG (181 GPa).[26] This implies that $BeAl_2O_4$ can be as robust a crystal as YAG and sapphire with excellent thermomechanical properties. No direct experimental data were found for the bulk modulus of $BeAl_2O_4$, although it was reported[29] that the Young's moduli for $BeAl_2O_4$ and α-Al_2O_3 are close and exceed 400 GPa. The Young's modulus depends on the crystal orientation and may even be sample dependent. On the other hand, the calculated B for YLF is only 90.0 GPa, less than half of $BeAl_2O_4$. This suggests that YLF is a much softer material and probably has a weaker electron-phonon interaction. Although we cannot find any direct measurement of bulk modulus for YLF, the elastic constants and Young's modulus for $LiCaAlF_6$ had been reported,[30] and are in the range of 100 GPa. Assuming these values are not too far from the bulk modulus and assuming YLF crystal is similar to $LiCaAlF_6$, then our calculated value of B for YLF is not inconsistent with these data. The relative softness of the fluoride laser materials implies some limitations in its applications when the hardness of the crystal is a crucial factor, such as the propensity for a laser crystal to shatter when experiencing thermal stress induced by strong optical pumping.

B. Band structure and density of states

The band structures and the density of states (DOS) of $BeAl_2O_4$ and $LiYF_4$ were calculated using the OLCAO method. Figures 3 and 4 show the band structures of the two crystals along the high-symmetry lines of the Brillouin zone (BZ). These band structures are typical of ionic insulators with relatively large band gaps and flat tops of the valence

TABLE II. Calculated ground-state and electronic properties of $BeAl_2O_4$ and $LiYF_4$. BW denotes the bandwidth in eV.

Crystal	$BeAl_2O_4$	$LiYF_4$
a (Å)	9.481	5.125
b (Å)	5.510	5.125
c (Å)	4.442	10.671
V/V_0	1.018	0.979
B (GPa)	217.2	90.0
B'	3.89	4.95
E_g (eV)	6.45	7.54
O/F $2p$ BW	7.73	3.16
O/F $2s$ BW	3.28	4.00

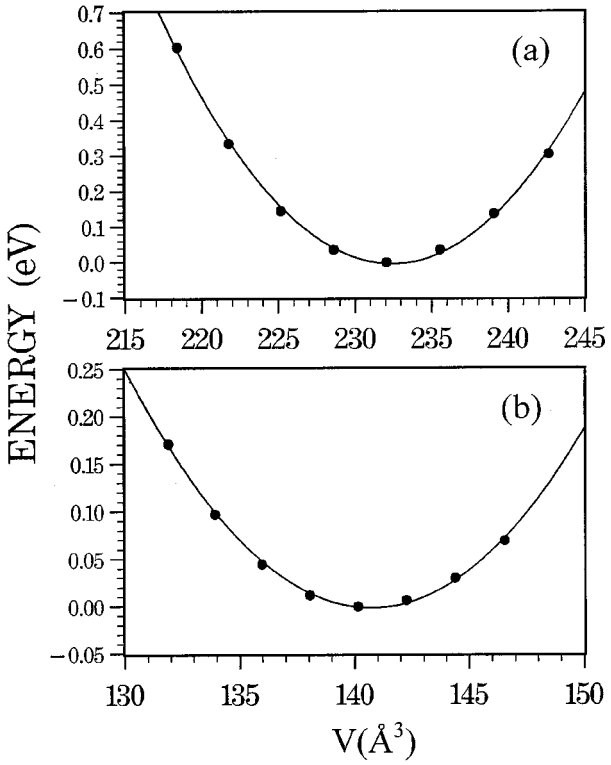

FIG. 2. Fitted E vs V curve for (a) $BeAl_2O_4$ and (b) $LiYF_4$.

band (VB). The gaps are direct, 6.45 eV for $BeAl_2O_4$ and 7.54 eV for $LiYF_4$. The real gaps may be even larger in both crystals since calculations based on LDA theory generally underestimate the band gaps of insulators. In both cases, the bottom of the conduction band (CB) is at Γ and consists of a single band.

The DOS and their partial atomic components (PDOS) of the two crystals are shown in Figs. 5 and 6. The VB of $BeAl_2O_4$ consists of two segments. The upper O $2p$ band is about 7.7 eV in width and the lower O $2s$ band is about 3.3 eV wide. The two segments are separated by a large gap of

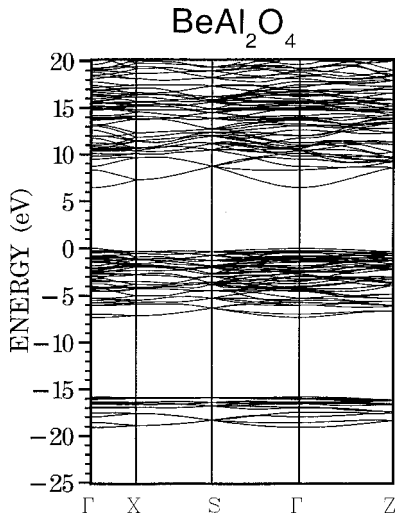

FIG. 3. Calculated band structure of $BeAl_2O_4$.

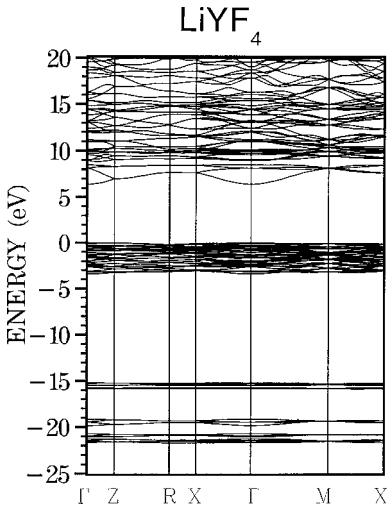

FIG. 4. Calculated band structure of $LiYF_4$.

almost 8.5 eV. A special point worth comment is that the PDOS of Be, Al1, and Al2 in $BeAl_2O_4$ are remarkably similar, differing only slightly in the 0.0 to -3.0 eV range. This is in spite of the fact that Be is tetrahedrally coordinated and Al's are octahedrally coordinated. Most likely, Be with one less valence electron than Al produces a similar local bonding structure as the Al at the octahedral site. The PDOS of O1, O2, and O3 in $BeAl_2O_4$ show some differences, especially with O3. This is because each O bonds to one Be and three Al ions. O1 and O2 each have two Al1 and one Al2 as

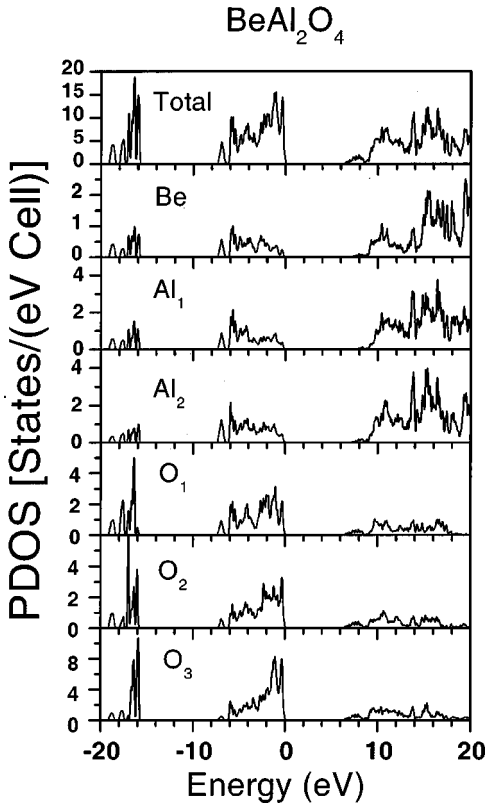

FIG. 5. Calculated total DOS and atom-resolved PDOS of $BeAl_2O_4$: (a) total; (b) Al1; (c) Al2; (d) Be; (e) O1; (f) O2; (g) O3.

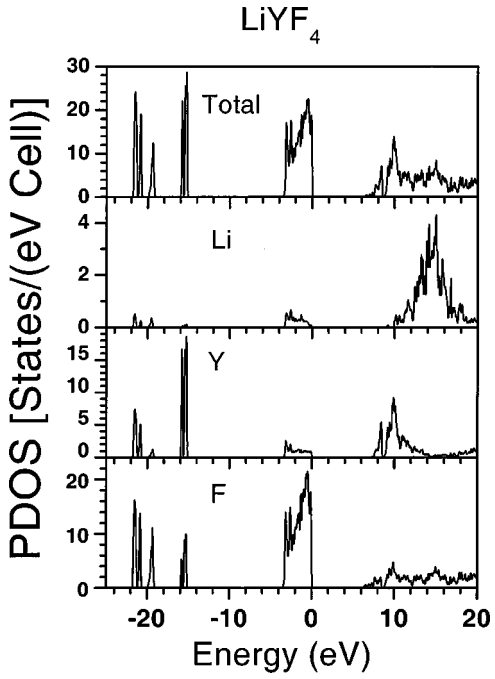

FIG. 6. Calculated total DOS and atom-resolved PDOS of $LiYF_4$: (a) total; (b) Li; (c) Y; (d) F.

NN's while O3 have two Al2 and one Al1 as NN's. There are differences in the bond lengths between Be, Al1, Al2, and the three O (see Table I).

The DOS and the PDOS of $LiYF_4$ are shown in Fig. 6 and they are quite different from that of $BeAl_2O_4$. The more ionic nature of $LiYF_4$ is very obvious. First, the gap is much larger and there are very little PDOS components from Li and Y ions in the upper VB. Most of the Li $2s$ valence electron, and to a lesser extent, the two Y $5s$ electrons and one Y $4d$ electron have been transferred to F. The upper VB derived from F $2p$ is very narrow, only 3.16 eV. It is separated from the much deeper F $2s$ and Y $4p$–derived bands by a large gap of 13.7 eV. The semi-core-like Y $4p$ levels interact rather strongly with the deep F $2s$ levels to produce two segments of bands centered at -20 and -17 eV in the deep VB. The lower one is dominated by F $2s$ states and the higher one by the Y $4p$ states. The significant interaction between F $2s$ and Y $4p$ orbitals has seldom been discussed in the literature and should not be overlooked. The lower part of the CB in YLF is mainly derived from the Y $4d$ orbitals.

C. Effective charge and bond order

The effective charges Q_α^* on each atom α and the bond order $\rho_{\alpha\beta}$ for each pair of atoms (α,β) in the crystal are calculated according to the Mulliken scheme:[31]

$$Q_\alpha^* = \sum_i \sum_{n,\mathrm{occ}} \sum_{j,\beta} C_{i\alpha}^{*n} C_{j\beta}^n S_{i\alpha,j\beta}, \tag{1}$$

$$\rho_{\alpha\beta} = \sum_{n,\mathrm{occ}} \sum_{i,j} C_{i\alpha}^{*n} C_{j\beta}^n S_{i\alpha,j\beta}. \tag{2}$$

TABLE III. Calculated effective charge Q_α^* in $BeAl_2O_4$ and $LiYF_4$. There are two Al sites and three O sites in $BeAl_2O_4$.

	$BeAl_2O_4$		$LiYF_4$
Be:	1.560	Li:	0.538
Al:	1.817, 1.786	Y:	1.837
O	6.721, 6.713, 6.702	F:	7.406

Here $C_{i\alpha}^n$ is the coefficient for the eigenvector for band n with atomic specification α and orbital specification i. $S_{i\alpha,j\beta}$ is the overlap matrix between the Bloch functions. Separate calculations using minimal basis sets were carried out for both $BeAl_2O_4$ and $LiYF_4$, since the Mulliken scheme is more meaningful when the basis functions are more localized. This is because the Mulliken scheme assumes equal partitioning of the overlap between two different atoms, which is true only for homopolar systems, and the error is accentuated when the basis functions are extended.

In the present calculation, 75 k points in the irreducible part of the BZ were used. The results are summarized in Table III. It shows that only 0.4 electron from Be and 1.2 electrons from Al are transferred to O in $BeAl_2O_4$. So, qualitatively speaking, there is a considerable covalent character in $BeAl_2O_4$ since there is only a partial charge transfer from the cation. In $LiYF_4$, about 0.5 electron from Li and 1.2 electrons from Y have been transferred to F and the charge transfer is also partial. (In this case, we did not include the semicore level of Y $4p$, which is assumed to have no charge transfer.) However, the Mulliken charge alone cannot accurately determine the ionicity of the crystal since Q^* is somewhat basis dependent. A more revealing factor will be the valence charge density distribution that will be discussed later.

The bond orders (BO's) between each pair of atoms in the two crystals calculated according to Eq. (2) are listed in Table IV. Also listed in parentheses are the corresponding interatomic distances. In $BeAl_2O_4$, the largest BO of 0.153 belongs to Be-O1 followed by 0.122 for Be-O3. The BO's of the Al-O pairs are slightly smaller. Thus our calculation shows that the Be-O bond is stronger than the Al-O bond in

TABLE IV. Calculated bond order $\rho_{\alpha,\beta}$ in $BeAl_2O_4$ and $LiYF_4$. The bond lengths in Å are listed in parentheses.

Crystal	$BeAl_2O_4$		$LiYF_4$
Be-O:	0.153 (1.579)	Y-F:	0.066 (2.244)
	0.107 (1.687)		0.057 (2.297)
	0.122 (1.631)		
Al1-O:	0.089 (1.861)	Li-F:	0.050 (1.897)
	0.089 (1.892)		
	0.094 (1.917)		
Al2-O:	0.077 (1.941)		
	0.106 (1.862)		
	0.077 (2.016)		
	0.106 (1.863)		
Al-Al:	0.041 (2.738)		

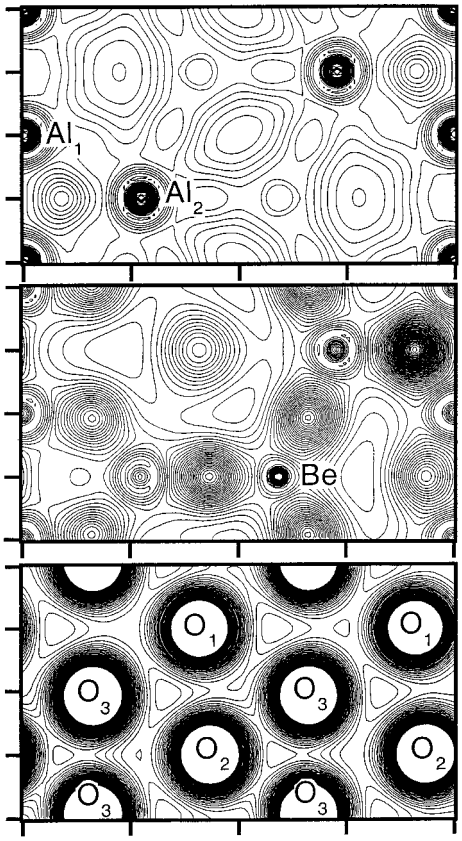

FIG. 7. Valence-charge-density contours in the (001) plane in $BeAl_2O_4$. The contour lines range from 0.00 to 0.25 electrons/(a.u.)^3 in intervals of 0.005. (a) $z/c=0$ plane showing Al1 and Al2; (b) $z/c=0.0665$ plane showing the Be ion; (c) $z/c=0.2585$ plane showing O1, O2, and O3. Note only O3 is exactly on this plane.

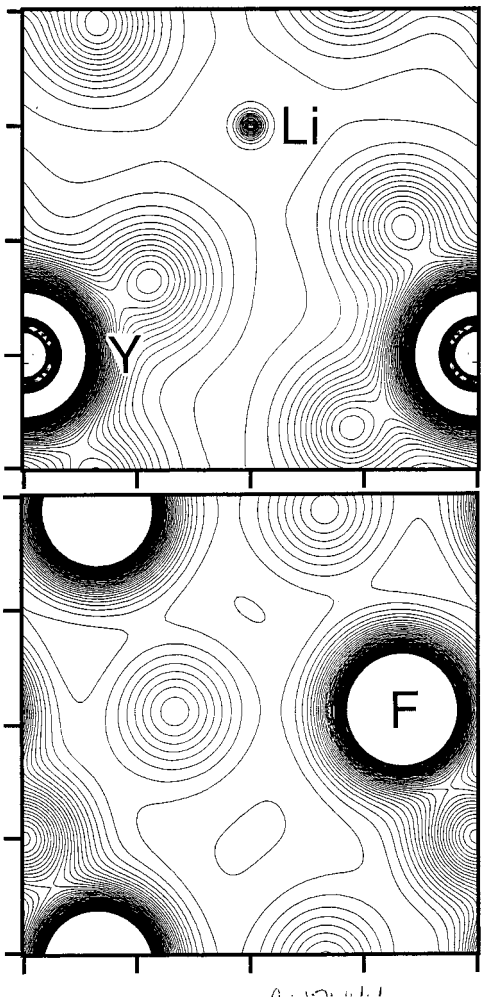

FIG. 8. (a) Valence-charge-density contours in the (001) plane in $LiYF_4$. The contour units are the same as in Fig. 6. (a) $z/c=0$ plane showing Li and Y; (b) $z/c=1.2937$ showing F ions.

this crystal even though Be is an element belonging to column II in the periodic table, which is generally believed to be more ionic. This is because of the substantially shorter BL for the Be-O pairs, ranging from 1.579 to 1.687 Å. It is also noted that the Al1-O3 pair with a BL of 1.917 Å has a BO of 0.094, larger than the BO of 0.089 for the Al1-O1 pair with a BL of 1.861 Å. Therefore, in this case, the BO does not strictly scale with the BL. Local symmetry and the presence of other nearby atoms can also influence the overall BO values. In $LiYF_4$ crystal, the BO of 0.05 between Li and F is much smaller, as is typical for alkali-metal ions. On the other hand, the BO of 0.083 for the Y-F pair is fairly large, considering the much larger distance of separation between the two ions. This is attributed to a considerable interaction of F $2s$ with the semicore Y $4p$ electrons discussed earlier.

D. Charge-density distributions

To illustrate more clearly the electronic structure and bonding in $BeAl_2O_4$ and $LiYF_4$ crystals, the valence charge distributions in these two crystals are shown in Figs. 7 and 8, respectively. Since there is no single crystallographic plane that contains all the cations and anions, several crystal planes perpendicular to the c axis are chosen. It can be seen that in $BeAl_2O_4$, the difference in the charge distribution between Al1 and Al2 in the $z=0$ plane is minimal. Figure 7(b) shows the charge distribution in the Be plane ($z/c=0.433$). Be is a much smaller ion but its bonding to O ions in the off-plane positions is quite obvious. Figure 7(c) shows the O3 plane ($z/c=0.259$), which also contains O1 and O2 in the slightly off-plane positions. The distributions of the charge around the O ions are nonspherical and show evidence of some covalent bonding with cations on the other planes.

The atomic arrangement in $LiYF_4$ is much more regular than in $BeAl_2O_4$. Figure 8(a) shows the charge distribution in the $z/c=0$ plane, which contains both cations. Li is a much smaller ion compared to Y. Bonding between Y and F ions on the other planes is evident. Figure 8(b) shows the charge distribution in the anion plane. The distribution of charges around the F ion is much more spherical than that around O in the $BeAl_2O_4$ crystal, indirectly supporting the viewpoint that YLF is more ionic.

V. CONCLUSIONS

We have studied the electronic structure and bonding in two laser crystals, $BeAl_2O_4$ and $LiYF_4$. We find that $LiYF_4$

is softer and more ionic than $BeAl_2O_4$. The electronic properties of $BeAl_2O_4$ resemble that of α-Al_2O_3 even though it contains tetrahedrally bonded Be atom. In $LiYF_4$, there is a significant interaction between the semi-core-like Y $4p$ electrons with F $2s$ orbitals, which contributes to the cohesion in the crystal. With the ground-state properties in these two crystals reasonably understood, the next logical step would be to study the specific dopant ions in these crystals and the resulting spectroscopic properties related to the laser performances. Such calculations have been attempted recently for Cr in YAG within framework of the one-electron theory.[32] It is conceivable that the theory may be extended to include the many-electron effects by direct calculation of the multiples using the one-electron result as a starting point.[15] We intend to study the Cr levels in $BeAl_2O_4$ using a supercell approach. It will be instructive to see if there are any spectroscopic differences for Cr substituting the Al1 or Al2 sites. Experimentally, it was found that about 70% of the Cr ions enter the Al1 site although the nature of the site preference is not clear.[20] The microscopic origin of the site preference in laser crystals is a problem of great importance.

For the $LiFY_4$ crystal, it would be desirable to study different rare-earth ions at the Y site since this is the main experimental interest. Such calculations will be much more demanding because the multiplet structures of rare-earth ions in a crystal field is much more complex than that of a transition-metal ion. It would also be of interest to see if excited-state absorption exists in these crystals.[33] Symmetry-allowed transitions from the doping levels in the gap to excited states either in the gap or to the conduction band have implications on the durability and stability of laser pumping, and also offer potential avenue for up-conversion channels in laser operation. Such studies can lead to a better understanding of the factors governing laser degradation and eventually improve their performances. Another area of significant interest is that the same fluoride crystals can be used as phosphor materials with very practical applications in the mercury-free fluorescent lamps and color plasma display panels.[34] In both $BeAl_2O_4$ and YLF, and in other laser crystals, one would eventually like to understand the roles of defects and the effect of ion-ion interaction based on a more realistic first-principles approach. Therefore, we expect fundamental studies in both the oxide and fluoride laser crystals will be an active area of research in years to come.

ACKNOWLEDGMENT

The work at UMKC was supported in part by the U.S. Department of Energy under Grant No. DE-FG02-84DR45170. The work of B.K.B. was supported in part by the U.S. Department of Energy under Contract No. DE-AC04-76-DP00613. W.Y.C. wishes to thank Dr. K. Orgasawara for helpful discussions. We thank Paul Rulis for assistance with graphics.

*Author to whom correspondence should be addressed. Electronic address: chingw@umkc.edu

[1] L. J. Atherton, S. A. Payne, and C. D. Brandle, Annu. Rev. Mater. Sci. **23**, 453 (1993).
[2] R. C. Powell, *Physics of Solid-State Laser Materials* (AIP Press, New York, 1997).
[3] J. S. Griffith, *The Theory of Transition Metal Ions* (Cambridge University Press, London, 1961).
[4] C. J. Ballhausen, *Introduction to Ligand Field Theory* (McGraw-Hill, New York, 1962).
[5] S. Sugano, Y. Tanabe, and H. Kamimura, *Multiplets of Transition Metal Ions in Crystals* (Academic, New York, 1970).
[6] Y.-N. Xu, W. Y. Ching, and B. K. Brickeen, Phys. Rev. B **61**, 1817 (2000).
[7] Y.-N. Xu and W. Y. Ching, Phys. Rev. B **59**, 10 530 (1999).
[8] W. Y. Ching, and Y.-N. Xu, J. Am. Ceram. Soc. **77**, 404 (1994).
[9] Y.-N. Xu and W. Y. Ching, Phys. Rev. B **43**, 4461 (1991).
[10] W. Y. Ching and Y.-N. Xu, Phys. Rev. B **59**, 12 815 (1999).
[11] F. Gan, M.-Z. Huang, Y.-N. Xu, W. Y. Ching, and J. G. Harrison, Phys. Rev. B **45**, 8248 (1992).
[12] N. C. Amaral, B. Baffeo, D. Guenzbur, Phys. Status Solidi B **117**, 141 (1983).
[13] J. Guo, D. E. Ellis, and D. J. Lam, Phys. Rev. B **45**, 3204 (1992).
[14] D. E. Ellis and J. Guo, J. Am. Ceram. Soc. **77**, 398 (1994).
[15] K. Ogasawara, T. Ishii, I. Tanaka, and H. Adachi, Phys. Rev. B **61**, 143 (2000).
[16] T. Ishii, K. Ogasawara, I. Tanaka, and H. Adachi, OSA Trends Opt. Photonics Ser. **34**, 514 (2000).
[17] J. C. Walling, D. F. Heller, H. Samelson, D. J. Harter, J. A. Pete, and R. C. Morris, IEEE J. Quantum Electron. **QE-21**, 1568 (1985).
[18] E. F. Farrell, J. H. Fang, and R. E. Newnham, Am. Mineral. **48**, 804 (1963).
[19] W. L. Bragg and G. B. Brown, Z. Kristallogr. **63**, 122 (1926).
[20] J. C. Walling, O. G. Peterson, H. P. Jenssen, R. C. Morris, and E. W. O'Dell, IEEE J. Quantum Electron. **QE-16**, 1302 (1980).
[21] E. Garcia and R. R. Ryan, Acta Crystallogr., Sect. C: Cryst. Struct. Commun. **49**, 2053 (1993).
[22] A. V. Goryunov, and I. Popov, Russ. J. Inorg. Chem. **37**, 126 (1992).
[23] W. Y. Ching, J. Am. Ceram. Soc. **71**, 3135 (1990).
[24] P. Hohenberg and W. Kohn, Phys. Rev. **136**, B864 (1964); W. Kohn and L. J. Sham, Phys. Rev. **140**, A1133 (1965).
[25] W. Y. Ching, L. Ouyang, J. D. Gale, Phys. Rev. B **61**, 8696 (2000).
[26] L. Ouyang and W. Y. Ching, J. Am. Ceram. Soc. (to be published).
[27] J. P. Perdew, in *Electron Structure of Solids '91*, edited by P. Ziesche and H. Eschrig (Akademie, Berlin, 1991), p. 11.
[28] F. D. Murnaghan, Proc. Natl. Acad. Sci. U.S.A. **30**, 244 (1944).
[29] W. F. Krupke, M. D. Shinn, J. E. Marion, J. A. Caird, and S. E. Stokowski, J. Opt. Soc. Am. B **3**, 102 (1986).
[30] B. W. Woods, S. A. Payne, J. E. Marion, R. S. Hughes, and L. E. Davis, J. Opt. Soc. Am. B **8**, 970 (1991).
[31] R. S. Mulliken, J. Chem. Phys. **23**, 1833 (1955).
[32] W. Y. Ching, Y.-N. Xu, and B. K. Brickeen, Appl. Phys. Lett. **74**, 3755 (1999).
[33] B. K. Brickeen and W. Y. Ching, J. Appl. Phys. **88**, 3073 (2000).
[34] See for example, *Phosphor Handbook*, edited by S. Shionoya and W. M. Yen (CRC, Boca Raton, 2000).